Eur. Phys. J. B **24**, 323–326 (2001)
DOI:

THE EUROPEAN PHYSICAL JOURNAL B
EDP Sciences

Nonlinear frequency conversion in 2D $\chi^{(2)}$ photonic crystals and novel nonlinear double-circle construction

Xue-Hua Wang[1] and Ben-Yuan Gu[2,a]

[1] Institute of Physics, Academia Sinica, PO Box 603, Beijing 100080, PR China

[2] CCAST (World Laboratory), PO Box 8730, Beijing 100080, PR China
and
Institute of Physics, Academia Sinica, PO Box 603, Beijing 100080, PR China

Received 19 April 2001

Abstract. The analytic solution to the wave equation for small-signal sum-frequency process is derived in 2D $\chi^{(2)}$ photonic crystals with use of the Green function method. It is predicted that the sum-frequency electrical field at quasi-phase matching (QPM) resonance is proportional to the angle-dependent effective crystal length. This implies that multiple wavelength QPM frequency conversion with controllable intensity output can be realized in a single 2D $\chi^{(2)}$ photonic crystal. It is revealed that efficient frequency conversion requires both the QPM and the proper structure matching. A novel double-circle construction, different from the conventional Ewald construction, is presented to reflect important QPM processes. It is also shown that the QPM resonance tuning of second-harmonic generation can operate over the whole transparent wavelength range of crystals.

PACS. 42.70.Qs Photonic bandgap materials – 42.65.Ky Harmonic generation, frequency conversion – 42.65.-k Nonlinear optics – 42.70.Mp Nonlinear optical crystal

Optical parametric processes are of importance for creating coherent sources at new frequencies where the conventional lasers perform poorly or are unavailable [1–6]. As is well-known, optical dispersion of crystals gives rise to different phase-velocities between interacting light waves with different frequencies. Then, efficient frequency conversion requires phase compensation for optical dispersion of crystals. Two schemes have been developed for this purpose. One is the critical phase-matching in the naturally or artificially anisotropic birefringent crystals [7–10]. But this is impossible for isotropic optical materials. Another is the quasi-phase-matching (QPM) in one-dimensional (1D) modulated nonlinear susceptibility structures [11–18]. However, the 1D structures severely limit the utilization of a single sample for frequency conversion. For example, it is very difficult for a single 1D QPM crystal to realize the multiple wavelength QPM frequency conversion with controllable intensity output and the QPM resonance tuning over the whole transparent wavelength region of the crystal.

Recently, 2D $\chi^{(2)}$ photonic crystals were proposed by Berger [19], in which nonlinear susceptibility $\chi^{(2)}$ varies periodically in the 2D plane, and the linear susceptibility $\chi^{(1)}$ is frequency-dependent, but position-independent. Last year, the first experimental sample is reported [20]. As compared to 1D case, new QPM processes with potential applications appear in the 2D plane, such as collinear QPM in multiple directions, multiple wavelength frequency conversion, multiple-beam second-harmonic generation (SHG) simultaneously in different directions, and ring cavity SHG. However, to our best knowledge, how to calculate the conversion efficiency in the 2D $\chi^{(2)}$ photonic crystals remains an open subject. In this paper, we present an analytic solution to wave equations for small-signal sum-frequency conversion in the 2D $\chi^{(2)}$ photonic crystals, and a novel double-circle construction different from the conventional Ewald construction for revealing new and important physical processes.

We now consider a 2D $\chi^{(2)}$ periodic array with enough large size poled in an infinite medium. This implies that a 2D $\chi^{(2)}$ crystal is embedded in an index matching background medium. Such a structure can be realized in $LiNbO_3$ or GaAs materials for extraordinary EM wave, as proposed by Berger [19]. Two elementary lattice vectors in 2D $\chi^{(2)}$ crystal are set to $\mathbf{a} = (a, 0)$ and $\mathbf{b} = (b_x, b_y)$, then the two primary reciprocal-lattice vectors are $\mathbf{G}_1 = \frac{2\pi}{a}(1, -\frac{b_x}{b_y})$ and $\mathbf{G}_2 = \frac{2\pi}{a}(0, \frac{a}{b_y})$. The numbers of unit cells along the $\mathbf{a}$ and $\mathbf{b}$ directions are denoted by N_a and N_b, respectively.

Without losing generality, we prefer to focus on the sum-frequency processes in the 2D $\chi^{(2)}$ crystals. In the

[a] e-mail: guby@aphy.iphy.ac.cn

small signal approach, power depletion of two pump light waves with frequencies of ω_1 and ω_2 and wave vectors of $\mathbf{k}_1$ ($k_1 = n(\omega_1)\omega_1/c$) and $\mathbf{k}_2$ ($k_2 = n(\omega_2)\omega_2/c$) may be neglected, *i.e.*, the magnitude of the two pump fields may be approximately considered as constants E_{10} and E_{20}. Then, the nonlinear wave equation of the sum-frequency field is reduced as

$$\nabla^2 E_3(\mathbf{r}) + k_3^2 E_3(\mathbf{r}) = -k_{30}^2 E_{10} E_{20} \chi^{(2)}(\mathbf{r}) \mathrm{e}^{\mathrm{i}\mathbf{k}\cdot\mathbf{r}}, \quad (1)$$

where $\mathbf{r} \equiv (x, y), k_{30} = \omega_3/c, k_3 = k_{30} n(\omega_3)$, and $\omega_3 = \omega_1 + \omega_2$; For convenience sake, hereafter $\mathbf{k} = \mathbf{k}_1 + \mathbf{k}_2$ is referred to as the "incident wave vector" and $\exp(\mathrm{i}\mathbf{k}\cdot\mathbf{r})$ as the "incident plane wave".

Using the Green function method [21] and considering the periodicity of $\chi^{(2)}(\mathbf{r})$, $E_3(\mathbf{r})$ can then be expressed as

$$E_3(\mathbf{r}) = \frac{1}{4\pi^2} \int_{-\infty}^{\infty} \mathrm{d}\mathbf{q} U(\mathbf{q}) \mathrm{e}^{\mathrm{i}\mathbf{q}\cdot\mathbf{r}}, \quad (2)$$

with

$$U(\mathbf{q}) = \frac{k_{30}^2 E_{10} E_{20} \Omega}{q^2 - (k_3 + \mathrm{i}\eta)^2} \chi^{(2)}(\mathbf{q} - \mathbf{k}) \times F(N_a, (\mathbf{q} - \mathbf{k})\cdot\mathbf{a}) F(N_b, (\mathbf{q} - \mathbf{k})\cdot\mathbf{b}), \quad (3)$$

$$\chi^{(2)}(\mathbf{q} - \mathbf{k}) = \frac{1}{\Omega} \int_{\Omega} \chi^{(2)}(\mathbf{r}') \mathrm{e}^{-\mathrm{i}(\mathbf{q}-\mathbf{k})\mathbf{r}'} \mathrm{d}\mathbf{r}';$$
$$F(N, \phi) = \frac{1 - \mathrm{e}^{-\mathrm{i}N\phi}}{1 - \mathrm{e}^{-\mathrm{i}\phi}}, \quad (4)$$

where η is a positive infinitesimal; Ω is the area of a unit cell, given by $\Omega = ab_y = \beta C_0^2$, C_0 denotes the lattice constant, and $\beta = 1, \sqrt{3}/2$, and $3\sqrt{3}/2$ for the square, triangular, and hexagonal lattices, respectively.

In general case, the analytical evaluation of the integral in equation (2) is impossibly drawn. However, if N_a and N_b are sufficiently large, we can obtain the explicit quasi-plane wave solution of $E_3(\mathbf{r})$ for two extreme cases: (i) $N_a \gg N_b$ and (ii) $N_b \gg N_a$. For this purpose, we rewrite equation (2) as follows

$$E_3(\mathbf{r}) = \int_0^{\infty} \frac{\mathrm{d}q}{4\pi^2} q \int_0^{\pi} \mathrm{d}\theta \, [U(\mathbf{q}) \mathrm{e}^{\mathrm{i}\mathbf{q}\cdot\mathbf{r}} + U(-\mathbf{q}) \mathrm{e}^{-\mathrm{i}\mathbf{q}\cdot\mathbf{r}}], \quad (\mathbf{q} = q(\cos\theta, \sin\theta)). \quad (5)$$

By inserting the well-known formula in solid physics

$$\lim_{N\to\infty} F(N, \phi) = 2\pi \sum_m \delta(\phi - 2m\pi), \quad (m = 0, \pm 1, ...)$$

into equation (5), we obtain the resulting expression for sum-frequency field $E_3(\mathbf{r})$ satisfying the (m, n)-order QPM condition

$$E_3(\mathbf{r}) = \mathrm{i} \frac{k_{30} E_{10} E_{20}}{2n(\omega_3)} \sum_{m,n} \chi^{(2)}(\mathbf{G}_{mn}) \times L_{\mathrm{eff}}^{(a)}(m, n) \mathrm{e}^{\mathrm{i}\mathbf{k}_{3,mn}\cdot\mathbf{r}} \delta_{\mathbf{k}_{3m}, \mathbf{k}_{3,mn}}, \quad (\text{for } N_a \gg N_b) \quad (6)$$

$$E_3(\mathbf{r}) = \mathrm{i} \frac{k_{30} E_{10} E_{20}}{2n(\omega_3)} \sum_{m,n} \chi^{(2)}(\mathbf{G}_{\mathrm{mn}}) \times L_{\mathrm{eff}}^{(b)}(m, n) \mathrm{e}^{\mathrm{i}\mathbf{k}_{3,mn}\cdot\mathbf{r}} \delta_{\mathbf{k}_{3n}, \mathbf{k}_{3,mn}}, \quad (\text{for } N_b \gg N_a), \quad (7)$$

where $\mathbf{k}_{3,mn} = \mathbf{k} + \mathbf{G_{mn}}$. In equations (6) and (7), $L_{\mathrm{eff}}^{(a)}(m, n) = N_b b \sin(\theta_b)/\sin\theta_{mn}$ and $L_{\mathrm{eff}}^{(b)}(m, n) = N_a a \sin\theta_b/\sin(\theta_b - \theta_{mn})$ are just the (m, n)-order QPM effective crystal length along the outgoing direction of the sum-frequency wave for $N_a \gg N_b$ and $N_b \gg N_a$, respectively, here, θ_b is the angle between the vector $\mathbf{b}$ and x axis. Note that θ_{mn} (or $\theta_b - \theta_{mn}$) is the angle between the outing direction and the vector $\mathbf{a}$ (or the angle between the outing direction and the vector $\mathbf{b}$). Hence, $L_{\mathrm{eff}}^{(a)}$ and $L_{\mathrm{eff}}^{(b)}$ are mathematically equivalent.

In general case, only a single order QPM resonance of $\mathbf{k}$ takes place. However, for some specific incident wave vectors, several different order QPM resonance may appear simultaneously in different directions on the 2D plane, in a similar way as the linear diffraction by a diffraction grating.

The above solutions show that the effective crystal length is angle-dependent, which becomes longer as the outgoing direction of the sum-frequency wave approaches the direction of the elementary lattice vector $\mathbf{a}$ (or $\mathbf{b}$). As compared to the 1D case, this provides a new and powerful route for enhancing conversion efficiency, and also indicates that the multiple wavelength frequency conversion with controllable intensity can be realized in a single 2D QPM crystal.

Note that the (m, n)-order QPM sum-frequency filed vanishes if the structural factor $\chi^{(2)}(\mathbf{G_{mn}}) = 0$. The corresponding structure is forbidden for the (m, n)-order QPM. So, the efficient frequency conversion requires not only the QPM but also the structure matching (SM) that corresponds to the maximum of $\chi^{(2)}(\mathbf{G_{mn}})$. As an example, we discuss the conditions of the "forbidden" and matching structures on 2D $\chi^{(2)}$ arrays consisting of circular cylinders. Assuming that $\chi^{(2)}(\mathbf{r}) = \chi_0^{(2)}$ (inside cylinders) or $-\chi_0^{(2)}$ (outside cylinders), then we obtain

$$\chi^{(2)}(\mathbf{G}_{mn}) = \frac{\chi_0^{(2)}}{\pi\beta\alpha_{mn}^2} x J_1(x), \quad (8)$$

where $x = G_{mn}R = 2\pi\alpha_{mn}R/C_0$, R is the radium of a circular cylinder; $\alpha_{mn} = \sqrt{m^2 + n^2 + mn}$ for the triangular and hexagonal lattices, while $\alpha_{mn} = \sqrt{m^2 + n^2}$ for the square lattice. Equation (8) shows that the "forbidden"

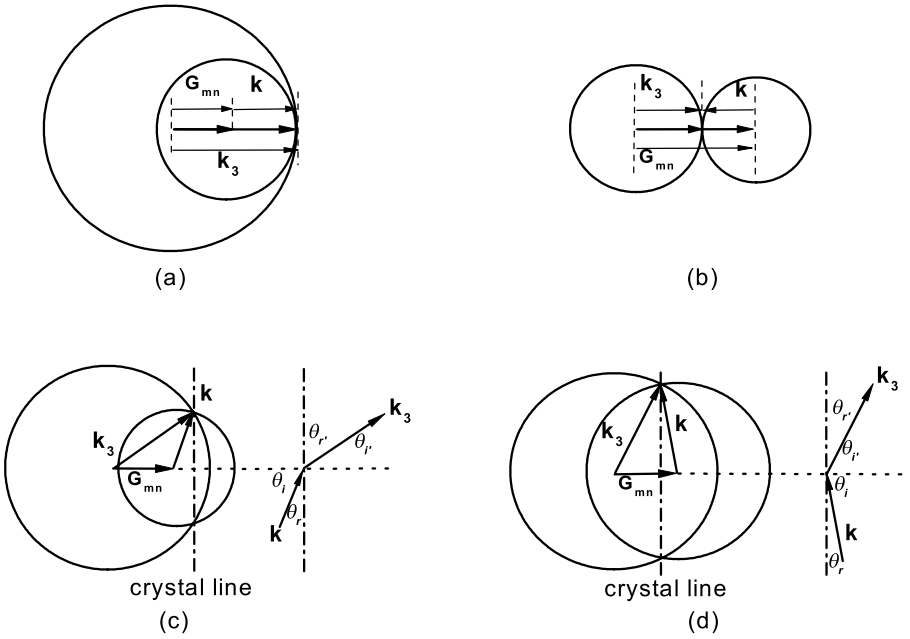

Fig. 1. Nonlinear double-circle construction: the centers of two circles are placed at the beginning and end points of a reciprocal vector $\mathbf{G}_{mn}$ and the radii of two circles are k_3 and k, respectively. There are four types of QPM processes: (a) the forward collinear QPM; (b) the backward collinear QPM (for clarity, the scale of G_{mn} has been enlarged); (c) "refraction" QPM; and (d) "reflection" QPM.

structures should satisfy

$$\frac{R}{C_0} = \frac{x_{1j}}{2\pi\alpha_{mn}}, \tag{9}$$

where $\{x_{1j}\}$ are the zero points of the first-order Bessel function. According to $\mathrm{d}(xJ_1(x))/\mathrm{d}x = xJ_0(x)$, the matching structures should satisfy

$$\frac{R}{C_0} = \frac{x_{0j}}{2\pi\alpha_{mn}}, \tag{10}$$

where $\{x_{0j}\}$ are the zero points of the zero-order Bessel function $J_0(x)$. It is noted that the ratio of R/C_0 can not exceed that of the close-packed structures. This gives rise to a finite number of matching structures. Then, the maximal x_{0J} defines the optimal matching structures of the (m,n)-order QPM in terms of equation (10).

As is well known, the conventional Ewald construction was used in searching for the Bragg diffraction in X-ray diffraction by crystals. Recently, it has been generalized to the 2D $\chi^{(2)}$ crystals in seeking for the QPM. However, the Bragg diffraction or the QPM is an "accidental-coincidence event" of this method. Here, we present a novel and heuristic double-circle construction for any order QPM, which can reveal many interesting physical processes associated with the QPM, as addressed below. The double-circle construction is described as follows: the centers of two circles are placed at the beginning and end points of the reciprocal vector $\mathbf{G}_{mn}$, and the radii of two circles are $k_3 = |\mathbf{k_3}|$ and $k = |\mathbf{k}|$, respectively. If there exists no any cross-point between two circles, the (m,n)-order QPM process is forbidden for the incident wave vector $\mathbf{k}$. Otherwise, this QPM process is allowed to happen. Moreover, it requires that $\mathbf{k}$ is along the direction of the link-line from the end point of $\mathbf{G}_{mn}$ toward the cross-point of two circles. Then, the sum-frequency wave propagates along the direction of the link-line from the beginning point of $\mathbf{G}_{mn}$ toward the cross-point. For "incident" wave vectors with different values of k, four types of the (m,n)-order QPM processes are found from this construction, as shown in Figure 1: (a) the forward collinear QPM with $k_3 - k = G_{mn}$; (b) the backward collinear QPM with $k_3 + k = G_{mn}$; (c) the "refraction" QPM in which the resonant sum-frequency field is similar to a refraction wave; (d) the "reflection" QPM in which the resonant sum-frequency field is similar to a reflected wave. For the cases of (c) and (d), there are two cross points between two circles. This indicates that there exist two equivalent incident directions for a given order non-collinear QPM. Thus, non-collinear QPMs are "double-degeneracy" at least.

Using some relationships in trigonal geometry, it easily deduces from Figure 1(c) that

$$k\sin\theta_i = k_3\sin\theta_{i'}, \tag{11a}$$

$$k_3\sin\theta_{r'} - k\sin\theta_r = G_{mn}. \tag{11b}$$

Equation (11a) shows that the "refraction" QPM is fully as like light refraction process at interface between two media. So, equation (11a) can be regarded as a *nonlinear Snell refraction law* in this process. From Figure 1(d), equation (11b) should be replaced by

$$k_3\sin\theta_{r'} + k\sin\theta_r = G_{mn}, \tag{11c}$$

which is then referred to as a *nonlinear Bragg reflection law* in "reflection" QPM process. In fact, if $k_3 = k = 2\pi/\lambda$, then $\theta_r = \theta_{r'} = \theta$ and equation (11c) is reduced to the well-known Bragg law in X-ray crystallography: $\lambda = 4\pi \sin\theta/G_{mn} = 2d_{mn}\sin\theta$, here d_{mn} is the space between crystal lines. Equation (11c) is more universal than equation (6) of reference [19]. In fact, for the SHG equation (11c) can be expressed in terms of the following form

$$\lambda_{2\omega} = \frac{2\pi}{G_{mn}}\left[\sin\theta_{r'} + \frac{n_\omega}{n_{2\omega}}\sin\theta_r\right] = \frac{2\pi}{G_{mn}}\sqrt{(1-\frac{n_\omega}{n_{2\omega}})^2 + 4\frac{n_\omega}{n_{2\omega}}\sin^2\frac{\theta_{r'}+\theta_r}{2}}.$$

By just setting $\theta_{r'} + \theta_r = 2\theta$, equation (6) of reference [19] is then obtained.

It is worthy to stressing that Figures 1(a) and (b) actually give the critical condition: $k_3 - k \leq G_{mn} \leq k_3 + k$ of the (m,n)-order QPM. This can be clearly seen in SHG process with $k = 2k_\omega = 4\pi n(\lambda)/\lambda$ and $k_3 = k_{2\omega} = 4\pi n(\lambda/2)/\lambda$, as shown below. In the general case, the optical dispersion of crystals has the properties of $n(\lambda_1/2) - n(\lambda_1) > n(\lambda_2/2) - n(\lambda_2)$ and $n(\lambda_1) > n(\lambda_2)$ if $\lambda_1 < \lambda_2$. So, $k_3 \pm k = G_{mn}$ gives rise to the resonant tuning wavelength range $\lambda_-^{(m,n)} \leq \lambda \leq \lambda_+^{(m,n)}$ for the (m,n)-order QPM SHG. It is determined by

$$\lambda_\pm^{(m,n)} = \frac{2C_0}{\alpha_{mn}}\left[n(\lambda_\pm^{(m,n)}/2) \pm n(\lambda_\pm^{(m,n)})\right]. \qquad (12)$$

It is noted that $\lambda_+^{(m,n)}/\lambda_-^{(m,n)} \gg 1$. This indicates that the QPM resonant tuning of the SHG in the 2D $\chi^{(2)}$ crystals may operate over the whole transparent wavelength range of crystals by adjusting the lattice constant C_0 and the QPM order α_{mn}.

In summary, We have presented a thoroughly theoretical analysis for the QPM processes in the 2D $\chi^{(2)}$ photonic crystals. The solution to the wave equation for small-signal sum-frequency process is derived by the Green function method. It is predicted that the conversion efficiency at the QPM is proportional to the square of the angle-dependent effective crystal length. This implies that the multiple wavelength frequency conversion with controllable intensity can be realized in a single 2D QPM crystal. It is also pointed out that efficient frequency conversion requires both the QPM and the proper structure matching. A novel double-circle construction different from conventional Ewald construction is presented. This construction reveals four types of the QPM processes, and shows that the 2D non-collinear QPM resonance follows nonlinear Snell refraction and Bragg reflection laws. Especially, it is demonstrated that the QPM resonant tuning of the SHG in the 2D $\chi^{(2)}$ photonic crystals may operate over the whole transparent wavelength range of crystals.

References

1. P.A. Franken, A.E. Hill, C.W. Petes, G. Weinreich, Phys. Rev. Lett. **7**, 118 (1961).
2. A. Yariv, P. Yeh, *Optic Wave in Crystal* (Wiley, New York, 1984).
3. Y.R. Shen, *The Principles of Nonlinear Optics* (Wiley, New York, 1984).
4. M.M. Fejer, G.A. Magel, D.H. Jundt, R.L. Byer, IEEE J. Quantum Electron. **28**, 2631 (1992).
5. N. Bloemberge, A.J. Sievers, Appl. Phys. Lett. **17**, 483 (1970); N. Bloembergenn, Phys. Today **45**, 28 (1993).
6. M.M. Fejer, Phys. Today **47**, 25 (1994); J.-P. Meyn, M.M. Fejer, Opt. Lett. **22**, 1214 (1997).
7. J.A. Giordmaine, Phys. Rev. Lett. **8**, 19 (1962).
8. P.D. Maker, R.W. Terhune, M. Nisenoff, C.M. Savage, Phys. Rev. Lett. **8**, 21 (1962).
9. J.P. Van Dex Ziel, Appl. Phys. Lett. **26**, 60 (1975).
10. A. Fiore, V. Berger, E. Rosencher, P. Bravetti, J. Nagle, Nature (London), **391**, 463 (1998).
11. J. Armstrong, N. Bloembergen, J. Ducuing, P.S. Pershan, Phys. Rev. **127**, 1918 (1962).
12. P.A. Franken, J.F. Ward, Rev. Mod. Phys. **35**, 23 (1963).
13. B.F. Levine, C.G. Bethea, R.A. Logan, Appl. Phys. Lett. **26**, 375 (1975); D.E. Thompson, J.D. Mcmullen, D.B. Anderson, *ibid.* **29**, 113 (1976).
14. M.S. Piltch, C.D. Cantrell, R.C. Sze, J. Appl. Phys. **47**, 3514 (1976); A. Szilagyi, A. Hordvik, H. Schlossberg, *ibid.* **47**, 2025 (1976).
15. L.E. Myers, G.D. Miller, R.C. Eckardt, M.M. Fejer, R.L. Byer, Opt. Lett. **20**, 52 (1995); L.E. Myers, R.C. Eckardt, M.M. Fejer, R.L. Byer, R.W. Bosenberg, J.W. Pierce, J. Opt. Soc. Am. B, **12**, 2102 (1995).
16. S.J.B. Yoo, C. Caneau, R. Bhat, M.A. Koza, A. Rajhel, N. Antoniades, Appl. Phys. Lett. **68**, 2609 (1996).
17. Y.Y. Zhu, N.B. Ming, Phys. Rev. B, **42**, 3676 (1990); S.N. Zhu, Y.Y. Zhu, Y.Q. Qin, H.F. Wang, C.Z. Ge, N.B. Ming, Phys. Rev. Lett. **78**, 2752 (1997).
18. S.N. Zhu, Y.Y. Zhu, N.B. Ming, Science **278**, 843 (1997).
19. V. Berger, Phys. Rev. Lett. **81**, 4136 (1998).
20. N.G.R. Broderick, G.W. Ross, H.L. Offerhaus, D.J. Richardson, D.C. Hanna, Phys. Rev. Lett. **84**, 4345 (2000).
21. K. Sakoda, K. Ohtaka, Phys. Rev. B **54**, 5742 (1996).